International Journal of Chemical, Materials and Biomolecular Sciences
ISSN: 2415-6620
Vol:8, No:7, 2014

The Effects of NaF Concentration on the Zinc Coating Electroplated in Supercritical CO_2 Mixed Zinc Chloride Bath

Chun-Ying Lee, Mei-Wen Wu, Li-Yi Cheng, Chiang-Ho Cheng

Abstract**—**This research studies the electroplating of zinc coating in the zinc chloride bath mixed with supercritical CO_2. The sodium fluoride (NaF) was used as the bath additive to change the structure and property of the coating, and therefore the roughness and corrosion resistance of the zinc coating was investigated. The surface characterization was performed using optical microscope (OM), X-ray diffractometer (XRD), and α-step profilometer. Moreover, the potentiodynamic polarization measurement in 3% NaCl solution was employed in the corrosion resistance evaluation. Because of the emulsification of the electrolyte mixed in Sc-CO_2, the electroplated zinc produced the coating with smoother surface, smaller grain, better throwing power and higher corrosion resistance. The main role played by the NaF was to reduce the coating's roughness and grain size. In other words, the CO_2 mixed with the electrolyte under the supercritical condition performed the similar function as brighter and leveler in zinc electroplating to enhance the throwing power and corrosion resistance of the coating.

Keywords**—**Supercritical CO_2, zinc-electroplating, sodium fluoride.

I. Introduction

DUE to its excellent corrosion protection capability, the zinc coating is frequently applied to improve the corrosion resistance of the substrate. Upon the exposure to corrosive atmosphere, a uniform and compact oxidized layer is formed on zinc surface, such as zinc oxide, zinc hydroxide, and zinc carbonate etc. This oxide film insulates the underneath zinc metal from further attack from the environment. Moreover, the zinc metal usually has higher electrode potential than the substrate it is designed to protect, which renders it as the anode when the oxide film is damaged and the outer atmosphere conducts current. Under this circumstance, the zinc metal acts as the sacrificial anode and protects the substrate, or the cathode, electrochemically [1]. For the preparation of zinc coating on iron substrate, both galvanized (EG) steel and electro-galvanized (CGI) steel can be used. However, the electrodeposition usually provides more flexibility in controlling the coating thickness and has better surface finish.

There are several plating systems which are widely used in industrial applications, for example, zinc sulfate bath, cyanide bath, zincate bath, and chloride bath, etc. The throwing power, limiting current density, and other properties are often employed to determine which bath system to be used [2]. However, they all belong to the conventional plating methods. Recently, Sone and co-workers proposed an emulsion plating method with the association of supercritical CO_2 [3]-[5]. The use of anionic surfactant and supercritical CO_2 formed the emulsion of supercritical CO_2 and electrolyte solution. The surface finish, grain size, pinhole populations, and hardness of nickel coating electrodeposited from this supercritical CO_2 emulsion method were greatly improved. Similar method was developed for the electrodeposition of copper for microelectronic applications [6]. Some other researchers also reported the effects of process parameters [7], the corrosion resistance [8], internal stress [9] of the Ni coating prepared in supercritical CO_2 mixed electrolyte. Apparently, the small supercritical CO_2 bubbles play an important role for the unique coating's properties. Based on the underlined mechanism of supercritical CO_2 plating, a post supercritical CO_2 assisted electrodeposition method was proposed and its effect was demonstrated [10].

Since the improvement in the surface finish and reduction in pinhole population can be beneficial to the corrosion protection performance, the adoption of supercritical CO_2 assisted electrodeposition for the preparation of zinc coating can be a viable attempt. Therefore, a zinc chloride bath with similar plating electrolyte in pH and temperature as the nickel bath was chosen as the deposition system. The effects of additives, such as NaF and wetting agent, on the prepared zinc coating were investigated.

II. Experimental

A. Materials

The chloride electrolyte bath adopted in this study was originally designed for the plating of strip and steel wire. In this case, the throwing power becomes less important because the surfaces have no recesses. The current efficiency and limiting current density will be more crucial to reduce the production cost. The bath contained zinc chloride ($ZnCl_2$, 150 g/L), sodium chloride (NaCl, 150 g/L), aluminum chloride ($AlCl_3$, 1.5 g/L) and sodium fluoride (2 ~ 16 g/L). The solution with highly polarizable chlorine ions had high conductivity and

C. Y. Lee is with the Department of Mechanical Engineering, National Taipei University of Technology, Taipei 10608, Taiwan (phone: +886-2-87731614; fax: +886-2-27317191; e-mail: leech@ntut.edu.tw).
M. W. Wu is with Chienkuo Technology University, Changhua 50015 (e-mail: mwwu@cc.ctu.edu.tw).
L. Y. Cheng was with Institute of Manufacturing Technology, National Taipei University of Technology, Taipei 10608, Taiwan (e-mail: chliyi@hotmail.com).
C. H. Cheng was with Department of Mechanical and Automation Engineering, Da-Yeh University, Changhua 51591, Taiwan (e-mail: chcheng@mail.dyu.edu.tw).

subsequently high limit current density. The addition of $AlCl_3$ in the electrolyte was to neutralize the effect of remnant iron ion during the pickling pretreatment before plating. However, the oxidation of ferric hydroxide and aluminum hydroxide produced flocculent precipitations in the electrolyte which was expensive to remove and could contaminate the deposited zinc at cathode. The existence of sodium fluoride in the bath further converted the ferrous ion salts into fluoride complexes, which was turned into crystalline compounds and formed sediment. All the chemicals were purchased with reagent grade and used without further refinement.

The substrate, placed at the cathode, was wire-cut 15 mm× 15mm carbon steel plate. The surface of the substrate was ground with 1500 grid emery paper, polished with 1μm alumina slurry, cleaned with de-ionized water, and activated with 20% HCl solution. In the anode, a piece of zinc plate was employed. For the supercritical CO_2 assisted plating, bottled dry ice grade CO_2 with 99.95% purity was used.

B. Electrodeposition Setup

The schematic diagram of the Sc-CO_2 electroplating system used in this work is depicted in Fig. 1. The reaction chamber, which had a volume of at.180 cc, was made of stainless steel with an inner Teflon lining for electrical insulation and chemical inertness. The underneath magnetic agitator and a surrounding temperature controlled water jacket were used for mixing and maintaining the constant temperature of the reaction chamber, respectively. The cathode was a 15 mm×15 mm iron plate and the anode was a zinc plate of the dimensions of 20mm×25mm×5mm. Both the cathode and anode were connected to the programmable DC power supply through titanium rods to the lead wires outside the chamber.

Prior to deposition, a fixed amount of electrolyte was put in the reaction chamber first. With the chamber cap closed, liquid CO_2 was introduced into the chamber using an air driven liquid pump, and the chamber was pressurized to a predetermined pressure. The solution was then agitated with a magnetic stirrer at a speed of 400 rpm for at least 30 min. before the electroplating process for solution stabilization and cathode cleaning. After plating, the cathode with zinc coating was rinsed in deionized water and then dried with warm stream of air.

C. Process Parameters

As mentioned previously, the electrolyte mainly contained $ZnCl_2$, NaCl, and $AlCl_3$. $6H_2O$. However, the content of NaF was adjusted in different levels: 0, 4, 8, and 12 g/L to investigate its effect on the prepared zinc coatings. Table I summarizes the process parameters employed in the deposition.

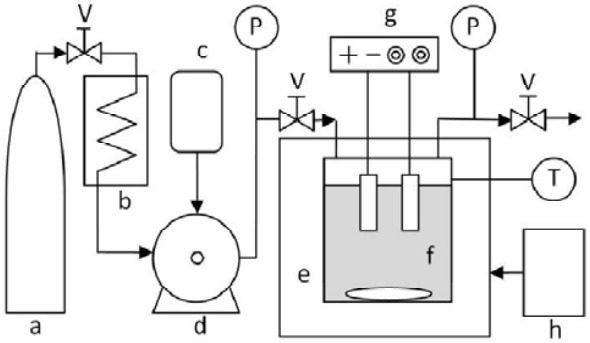

Fig. 1 The schematic diagram for the setup of supercritical CO_2 assisted electrodeposition: (a) CO_2 bottle, (b) cooler, (c) air compressor, (d) high pressure liquid pump, (e) hot water jacket, (f) bath container with magnetic stirrer, (g) DC power supply, (h) hot water reservoir, (P) pressure gauge, (V) pressure valve, (T) thermometer

TABLE I
PROCESS PARAMETERS USED IN THE ELECTRODEPOSITION

parameter	magnitude	
Current density (A/dm^2)	3	
Nominal thickness (μm)	10	
Plating process	Conventional	Supercritical-CO_2
Temperature (°C)	20~25	40
Pressure (MPa)	0.10	8.27
NaF concentration (g/L)	0, 4, 8, 12	
Wetting agent (mL/L)	0, 1, 2	
pH	4.8~5.4	

D. Microstructure Examination

The surface morphology of the specimen was examined by a scanning electron microscope (SEM), the JEOL-JSM-7401F. The average grain size of deposits was measured by the X-ray Diffraction (XRD), MAC Science M03XHF X-ray diffractometer, at a sweeping rate of 2 deg/min and calculated by the Scherrer equation. The X-ray was generated by a Cu-K_α target operated at 30 kV and 20 mA with a wavelength of 0.15418 nm. The surface roughness measurement of the coating was performed at ten different sweeps over vertical and horizontal directions of each sample using a profilometer, KOSAKA Surfcorder SEF3500a. Finally, the polarization curves were obtained from a potentiostat, Jichen Electrochemical Workstation-5000.

III. RESULTS AND DISCUSSION

A. Current Efficiency

The current efficiency of the electrodeposition in electrolyte with different NaF concentrations is presented in Fig. 1. The conventional plating had current efficiency higher than 95% which was high among all feasible Zn plating baths. It is clearly seen that the conventional process had higher current efficiency than the supercritical CO_2 assisted ones. The chloride bath used in this study had very high current efficiency. However, the mixing of supercritical CO_2 bubbles in the electrolyte can lower the electrical conductivity of the bath and carry away the reduced hydrogen bubbles easily. Thus, a lower current

efficiency was observed. The addition of NaF into the electrolyte had slightly more improvement on the current efficiency for the supercritical CO_2 process than the conventional one. The NaF had emulsifying function to some extent such that it can reduce the size of the CO_2 bubbles and improve the conductivity of the electrolyte.

The further addition of wetting agent ($CH_3(CH_2)_{11}SO_4Na$) into the electrolyte containing 8 g/L of NaF influenced the current efficiency and the result is shown in Fig. 2. The wetting agent was able to reduce the surface tension of the electrolyte and improve the wetting of cathode. Thus, the bubble of reduction reaction can easily escape from the cathode surface and reduce the formation of pinhole in the coating. However, the current efficiency was slightly decreased with the addition of wetting agent. On the other hand, the addition of 1 mL/L wetting agent into the electrolyte for the supercritical CO_2 plating caused a small increase in the current efficiency. But a slight decrease in current efficiency was observed with further increase in the concentration of wetting agent to 2mL/L. It was suspected that the wetting agent still contributed to the well dispersion of the CO_2 bubbles in the electrolyte. However, as more wetting agent was added, the dispersion function saturated and the decrease in electrical conductivity reversed the trend in the improvement of current efficiency.

A. Surface Morphology and Roughness

Fig. 4 presents the photographs of the specimen surfaces prepared in conventional and supercritical CO_2 processes, respectively, taken from optical microscope. It is obviously seen that the supercritical method prepared the coating with more uniform surface coverage. Moreover, the addition of more NaF clearly improved the surface uniformity. The use of wetting agent, on the other hand, also improved the surface uniformity, as seen in Fig. 5.

The associated surface roughness for the prepared coating was presented in Fig. 6. For both conventional and supercritical processes, the surface roughness of the prepared coatings was improved with the amount of NaF added to the electrolyte. In accordance with the surface morphology observed in Fig. 4, the supercritical CO_2 process prepared the coating with better surface finish. It is noted that without NaF, the coating prepared with conventional process showed big variation which was consistent with the poor uniformity in the OM examination.

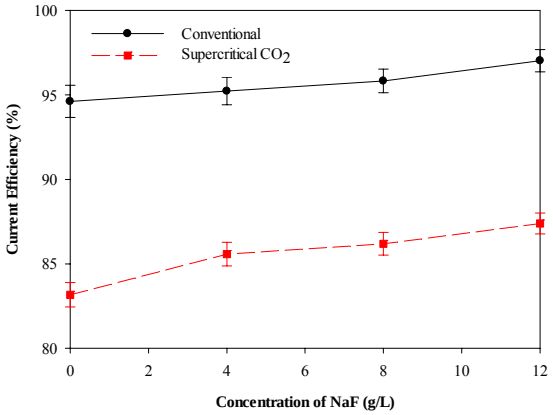

Fig. 2 The current efficiency of the electrodeposition in electrolyte with different NaF concentrations

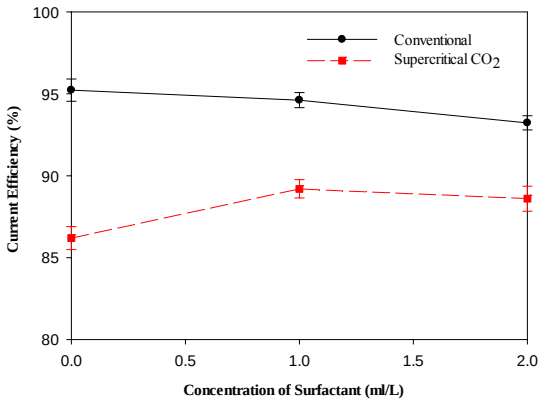

Fig. 3 The current efficiency of the electrodeposition in electrolyte containing 8 g/L of NaF and with different surfactant concentrations

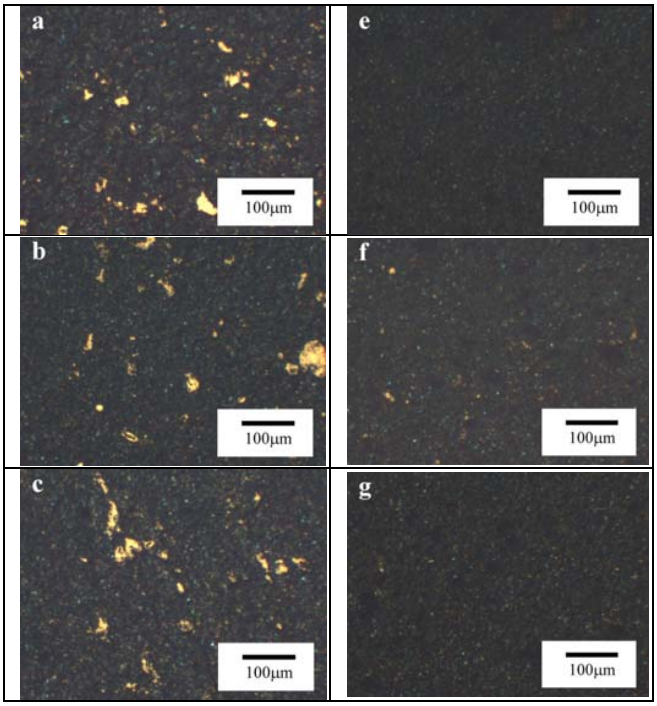

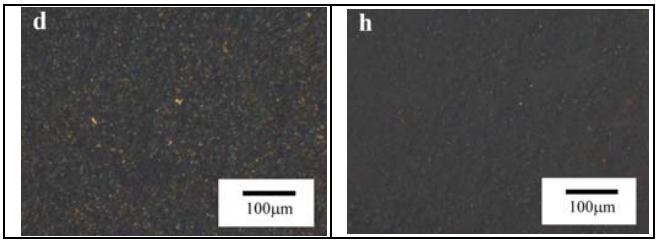

Fig. 4 The OM surface photographs of coatings prepared from different electrolytes containing different concentrations of NaF: conventional (a) 0 g/L (b) 4 g/L (c) 8 g/L (d) 12 g/L; supercritical CO_2 (e) 0 g/L (f) 4 g/L (g) 8 g/L (h) 12 g/L

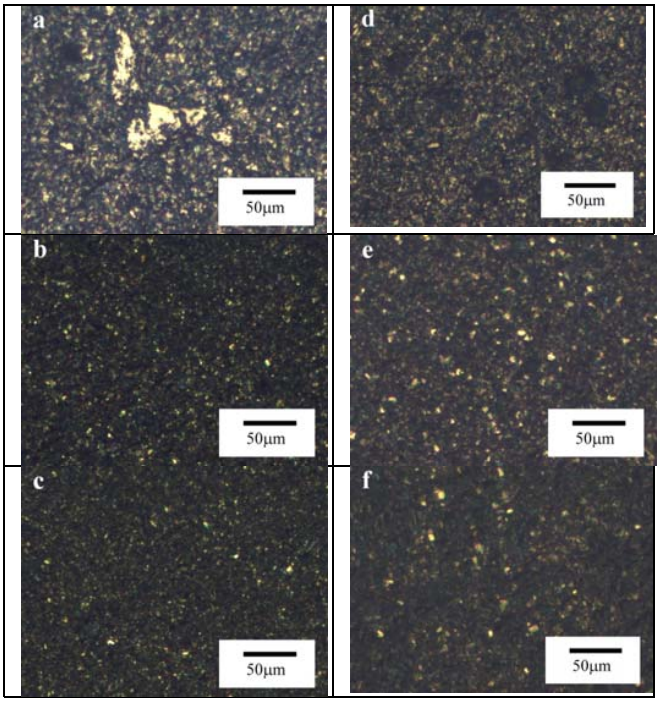

Fig. 5 The OM surface photographs of coatings prepared from electrolyte containing 8 g/L NaF and different amounts of wetting agent: conventional (a) 0 g/L (b) 1 mL/L (c) 2 mL/L; supercritical CO_2 (d) 0 mL/L (f) 1 mL/L (e) 2 mL/L

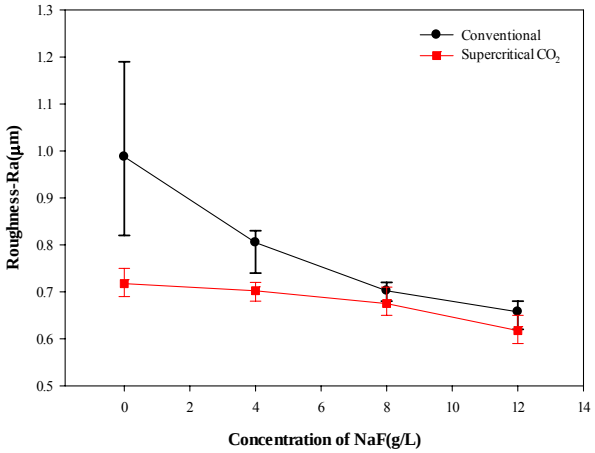

Fig. 6 The measured surface roughness of coatings prepared from electrolytes with different NaF concentrations

B. Microstructure

Fig. 7 presents the measured X-ray diffraction spectra for the coatings prepared from two different processes and with different NaF concentrations. It is noted that without NaF in the electrolyte, the prepared coatings from both processes showed a strong texture of (0002). However, the addition of NaF to the electrolyte diminished the dominance of (0002) and the emergence of $(10\bar{1}1)$ occurred. According to the Scherrer formula, the calculated grain size from (0002) peak is shown in Table II. The grain refining due to the presence of NaF was observed for both processes. Moreover, the supercritical CO_2 process added to the further reduction in grain size.

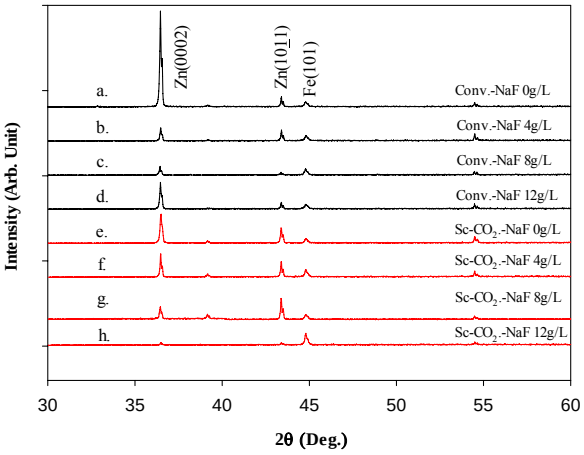

Fig. 7 The X-ray diffraction spectra for coatings prepared from both conventional and supercritical processes, respectively, and with different NaF concentrations.

TABLE II
CALCULATED GRAIN SIZE FROM THE (0002) DIFFRACTION PEAK FOR COATINGS PREPARED IN DIFFERENT NAF CONCENTRATIONS

Plating Process	Concentration of NaF (g/L)			
	0	4	8	12
Conventional	139.5nm	69.7nm	54.0nm	52.3nm
Supercritical-CO_2	93.0nm	64.3nm	46.5nm	41.8nm

C. Polarization Curve

Fig. 8 presents the measured polarization curves of the coatings prepared with conventional plating process in different NaF concentrations. From these polarization curves, the corresponding corrosion potential (E_{corr}) and corrosion current (i_{corr}) can be obtained and they are listed in Table III, along with those measured from the coatings prepared by supercritical CO_2 process. From the results presented in Table III, it is seen that coatings prepared from supercritical CO_2 process had slightly higher corrosion potential that their conventional counterparts. Moreover, the corrosion current density was all lower for the coatings prepared from the supercritical CO_2 process. Therefore, the zinc coating electrodeposited from supercritical CO_2 process was slightly improved in corrosion resistance. Nevertheless, with the increase in NaF concentration, the grain size, presented in Table II, was decreased correspondingly. Usually, the grain boundary is the region having higher activated energy and showed high corrosion activity. Therefore, the reduction in grain size resulted in the increase in corrosion current. On the other hand, the (0002) crystalline plane is the most packed one in the crystalline structure and assumes better corrosion resistance to other planes. Fig. 7 showed that the (0002) texture was diminished as the concentration of NaF increased. This also contributed to the increase in corrosion current as the NaF concentration was raised.

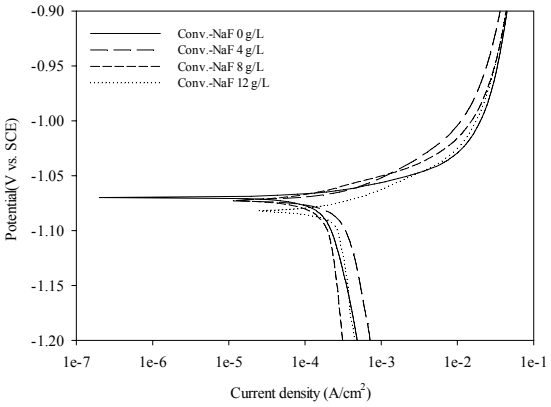

Fig. 8 The measured polarization curves of the coatings prepared with conventional plating in electrolytes with different NaF concentrations

TABLE III
THE CORROSION POTENTIAL AND CORROSION CURRENT FOR COATINGS PREPARED IN ELECTROLYTE WITH DIFFERENT NAF CONCENTRATIONS

	Concentration of NaF (g/L)							
	0		4		8		12	
	Conv.	Sc-CO_2	Conv.	Sc-CO_2	Conv.	Sc-CO_2	Conv.	Sc-CO_2
E_{corr} (V)	-1.07	-1.04	-1.07	-1.05	-1.08	-1.02	-1.08	-1.05
I_{corr} (A/m^2)	1.89	1.55	2.30	1.67	2.53	1.33	2.80	1.83

Furthermore, the effect of wetting agent on the corrosion resistance of the prepared coatings is depicted in Table IV. As the concentration of wetting agent increased, the corrosion potential remained nearly unchanged, while the corrosion current decreased significantly. Again, the coating prepared from supercritical CO_2 process demonstrated better corrosion resistance than the conventional process.

TABLE IV
THE CORROSION POTENTIAL AND CORROSION CURRENT FOR COATINGS PREPARED IN ELECTROLYTE WITH 8 G/L NAF AND DIFFERENT SURFACTANT CONCENTRATIONS

Process	Surfactant(mL/L)	E_{corr}(V)	i_{corr}(A/m^2)
Conventional	0	-1.079	2.53
	1	-1.009	1.27
	2	-1.006	1.22
Supercritical CO_2	0	-1.017	1.33
	1	-1.001	0.967
	2	-1.000	0.675

The corrosion resistance of the zinc coating was further examined by immersion testing in 3.5% NaCl solution. The result was represented by the corrosion penetration rate (CPR) as following:

$$CPR = \frac{KW}{T\rho A}, \quad (1)$$

where W was the weight loss during immersion, T denoted the immersion period (hour), ρ was the mass density of the coating, A was the exposed surface area of the specimen. If mm/yr was employed as the unit of CPR, the constant K can be determined and (1) can be written as

$$CPR(mm/yr) = \frac{87.6W}{T\rho A} \quad (2)$$

For the coatings immersion tested in 3.5% NaCl solution, their CPR changes with the immersion time are presented in Fig. 9. Overall speaking, the CPR first increased and then decreased with the immersion time. The formation of corrosion product film on the surface should be crucial for this gradual decrease in CPR. In addition, the coatings prepared from the conventional process demonstrated higher CPR than their Supercritical CO_2 counterparts. The trend was consistent with the corrosion current results found in Table III. The higher corrosion weight loss for conventional plating might relate to the higher surface roughness than its supercritical CO_2 counterpart.

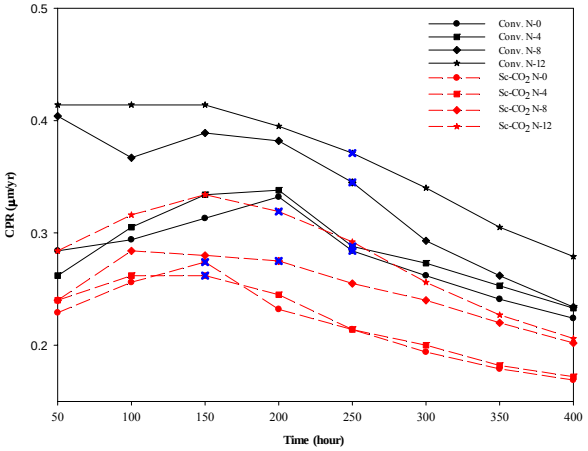

Fig. 9 The corrosion rate of CPR for the coatings immersed in 3.5% NaCl solution

IV. Conclusion

As an additive in the zinc plating bath, NaF can dissolve in the electrolyte easily. Because the fluorine has small atomic size and high electronegativity, the dissolved fluoride ion has high surface activity and lowers the surface tension of the solution. The accompanying emulsifying function of NaF reduced the surface roughness and grain size of the Zn coating. Although the smoother surface could improve its corrosion resistance, grain refining generated more grain boundary domain and dominated the worsening of the corrosion resistance of the coating. In addition, the change of crystalline texture from (0002) to $(10\bar{1}1)$ may also contribute to the reduction in corrosion resistance. Thus, the raise of the NaF concentration in the conventional plating bath produced coating with lower corrosion resistance. On the other hand, the use of supercritical CO_2 plating process helped to prepare the coating with finer grain and greatly smooth surface. The addition of NaF in supercritical CO_2 plating further smoothed the surface and refined the grain. Therefore, an improvement in corrosion resistance of Zn coating by using supercritical CO_2 plating process was obtained. In spite of the use of wetting agent could obtained similar improvement in the corrosion resistance of the prepared coating, the concern of incorporating impurity elements, such as sulfur, in the coating can be alleviated by employing supercritical CO_2 process.

Acknowledgment

The financial support from National Science Council, Taiwan, under Grant No. NSC 102-2221-E-027-020 is gratefully acknowledged.

References

[1] M. G. Fontana, and N. D. Greene, *Corrosion Engineering*, 3rd ed., New York: McGraw-Hill, 1986.
[2] F. A. Lowenheim, *Modern Electroplating*, 3rd ed., New York: John-Wiley, 1963.
[3] H. Yoshida, M. Sone, A. Mizushima, K. Abe, X.T. Tao, S. Ichihara, S. Miyata, "Electroplating of nanostructured nickel in emulsion of supercritical carbon dioxide in electrolyte solution," Chemistry Letters, vol. 11, pp. 1086-1087, 2002.
[4] T.F.M. Chang, M. Sone, A. Shibata, C. Ishiyama, Y. Higo, "Bright nickel film deposited by supercritical carbon dioxide emulsion using additive-free Watts bath," Electrochimica Acta, vol. 55, pp. 6469-6475, 2010.
[5] T.F.M. Chang, M. Sone, "Function and mechanism of supercritical carbon dioxide emulsified electrolyte in nickel electroplating reaction," Surface and Coatings Technology, vol. 205, pp. 3890-3899, 2011.
[6] N. Shinoda, T. Shimizu, T.F.M. Chang, A. Shibata, M. Sone, "Filling of nanoscale holes with high aspect ratio by Cu electroplating using suspension of supercritical carbon dioxide in electrolyte with Cu particles," Microelectronic Engineering, vol. 97, pp. 126-129, 2012.
[7] M. S. Kim, J. Y. Kim, C. K. Kim, and N. K. Kim, "Study on the effect of temperature and pressure on nickel-electroplating characteristics in supercritical CO_2," Chemosphere, vol. 58, pp. 459-465, 2005.
[8] S.T. Chung, H.C. Huang, S.J. Pan, W.T. Tsai, P.Y. Lee, C.H. Yang, M.B. Wu, "Material characterization and corrosion performance of nickel electroplated in supercritical CO_2 fluid," Corrosion Science, vol. 50, pp. 2614-2619, 2008.
[9] V.C. Nguyen, C.Y. Lee, F.J. Chen, C.S. Lin, T.Y. Liu, "Study on the internal stress of nickel coating electrodeposited in an electrolyte mixed with supercritical carbon dioxide," Surface and Coatings Technology, vol. 206, pp. 3201-3207, 2012.
[10] C. V. Nguyen, C. Y. Lee, F. J. Chen, C. S. Lin, L. Chang, "An Electroplating Technique using the Post Supercritical Carbon Dioxide Mixed Electrolyte," Surface & Coatings Technology, vol. 232, pp.234-239, 2013.